IOP Publishing Measurement Science and Technology
Meas. Sci. Technol. 31 (2020) 045001 (15pp) https://doi.org/10.1088/1361-6501/ab50aa

Distinguish coherence resonance and stochastic resonance in bearing fault evaluation

Chen Yang[1,2], Jianhua Yang[1,2,4], Zhencai Zhu[1], Gang Shen[1] and Yuqiao Zheng[3]

[1] School of Mechatronic Engineering, China University of Mining and Technology, Xuzhou 221116, People's Republic of China
[2] Jiangsu Key Laboratory of Mine Mechanical and Electrical Equipment, China University of Mining and Technology, Xuzhou 221116, People's Republic of China
[3] School of Mechanical and Electronic Engineering, Lanzhou University of Technology, Lanzhou 730050, People's Republic of China

E-mail: jianhuayang@cumt.edu.cn

Received 29 August 2019, revised 10 October 2019
Accepted for publication 23 October 2019
Published 6 January 2020

Abstract

Similar to the famous stochastic resonance (SR), coherence resonance (CR) is an ordered dynamic behavior induced by the noise in a nonlinear system. Inspired by the dynamical characteristics of CR, the importance of distinguishing CR and SR in bearing fault evaluation is presented. It solves the problem that the characteristic frequency cannot be determined when using the SR for bearing fault diagnosis. The general scale transformation is introduced to process the vibration signal further to realize adaptive CR at different frequencies. The autocorrelation function and the resonance factor are key measurements of CR. Especially, the resonance factor index can reflect the output of the nonlinear system transforming from CR to SR and then realize the detection of the characteristic frequency and then identify the bearing fault. Numerical and experimental verifications show the advantages of the CR method in the periodic potential system in bearing fault diagnosis are illustrated. By distinguishing CR and SR successfully, we can improve the accuracy of bearing fault diagnosis.

Keywords:coherence resonance, stochastic resonance, fault diagnosis, autocorrelation function, resonance factor

(Some figures may appear in colour only in the online journal)

1. Introduction

Rolling bearings, as the core components of rotating machinery, are the basic components to ensure the normal operation of the equipment, which are usually subjected to strong loads [1]. If the bearing fails, it will easily cause the equipment to stop running, resulting in casualties. Therefore, implementing bearing fault evaluation methods is important for monitoring bearing status and reliability. At present, the common fault diagnosis process includes: pre-processing bearing vibration signal, using a variety of methods [2–4] to extract fault features and realize fault mode diagnosis. Among them, extracting fault features is the key to realizing fault diagnosis. However, due to the influence of complex working conditions and mechanical transmission path, the collected vibration signals are disturbed by strong noise, which greatly increases the difficulty of feature extraction.

According to the processing method of background noise, the common fault feature extraction methods can be classified. Some methods [5–8] regard noise as totally harmful and try to filter out noise as much as possible to improve the signal-to-noise ratio (SNR). For example, Yang *et al* proposed a bearing

[4] Author to whom any correspondence should be addressed.

fault diagnosis method based on EMD energy entropy [9]. Lou *et al* applied wavelet transform and neuro-fuzzy classification to bearing fault pattern recognition [10]. However, it is worth noting that the above methods will inevitably filter out some weak feature information, resulting in the false impression of improving the SNR. In contrast, some reports [11–15] have proved that stochastic resonance (SR) has the unique advantage of using harmful background noise to enhance weak characteristic signals through a non-linear system. Therefore, many methods based on SR theory are widely used in bearing fault diagnosis [16–19]. Coherence resonance (CR) [20–25] also has the ability to transform noise energy to a certain frequency. Different from SR, CR occurs in a noise-driven excitable system [26], which does not require the participation of characteristic excitation. For an appropriate noise intensity, the output of the non-linear system will show ordered performance, and the frequency spectrum of CR is similar to that of SR. CR has been investigated theoretically in many fields, but there is little report on CR in engineering applications.

Based on SR method to enhance feature information and realize fault diagnosis, it is necessary to know the fault type of bearing in prior. However, for the bearing vibration signals collected on site, the fault is usually unknown. To solve this problem, a novel method of judging SR and CR will be provided to detect a weak characteristic signal. If we do not distinguish SR and CR, we may extract imaginary frequency by inducing CR, and the output of the system still appears to be a resonance phenomenon even if the bearing is in health. This brings interference to the bearing fault diagnosis. As a result, how to accurately identify SR and CR is the key problem of bearing fault evaluation.

Aimed at the above problems of bearing fault diagnosis, a new method based on CR is proposed in this paper, which evaluates the bearing fault and improves the accuracy of bearing fault detection. Firstly, due to the advantages of the periodic potential system in computing speed and improving SNR [27, 28], the existence of CR is proved by combining the general scale transformation method [29] with the periodic potential system through the system output. Furthermore, the autocorrelation function [26] is introduced to study and analyze the coherence of the system output. At the same time, the difference between CR and SR is highlighted by comparing the output of the autocorrelation function. In order to make the results more intuitive, the resonance factor index is constructed, which reflects the transformation from CR to SR from the numerical value and evaluates the bearing fault.

This paper is outlined as follows. Section 2 mainly introduces CR and corresponding indicators proposed in this paper. Section 3 evaluates the effectiveness of the proposed method by using bearing fault simulation signals. Section 4 deals with the experimental signal. The quantization of CR is successfully realized by using the resonance factor index. The applicability of the novel method in bearing fault evaluation is verified. The advantage of the periodic potential system over the bistable system is verified by the experimental signal. Finally, the main conclusions of this paper are given in section 5.

2. Theoretical formulation

Both CR and SR are noise-induced ordered phenomenon in nonlinear systems. However, the former phenomenon does not need the cooperation of weak character signal. Under a certain noise intensity, the regularity of the system output achieves the greatest degree. In contrast, SR needs the participation of weak characteristic signal. Generally speaking, SR can be regarded as a special case of CR. The following is a description of the CR model.

2.1. Adaptive CR

CR can be interpreted as the quasi-periodic transition of the Brownian particle driven by noise between potential wells. We investigate CR by using the following equation:

$$\begin{cases} \frac{\mathrm{d}x}{\mathrm{d}t} = -U'(x) + N(t) \\ \langle N(t)\rangle = 0, \langle N(t+\tau)N(t)\rangle = 2D\delta(\tau) \end{cases} \tag{1}$$

where $N(t)$ is the Gaussian white noise with intensity D, $\delta(t)$ is the delta function, $U(x)$ is the potential function. For the periodic potential system, $U(x)$ can be expressed as

$$U(x) = -a\cos(bx). \tag{2}$$

Therefore, the CR model represented by equation (1) can be written as

$$\begin{cases} \frac{\mathrm{d}x}{\mathrm{d}t} = -ab\sin(bx) + N(t) \\ \langle N(t)\rangle = 0, \langle N(t), N(0)\rangle = 2D\delta(t) \end{cases} \tag{3}$$

where $a > 0$ and $b > 0$ denote the barrier parameters of the periodic potential. Specifically, a and b influence the height of the barrier and the width between two adjacent stable equilibriums. Different from the famous SR model, the periodic signal $s(t)$ is absent in the equation. To achieve CR or SR at a high frequency, we need to find the appropriate system parameters [30]. Referring to the general scale transformation SR method, we adopt the variable transformations

$$x(t) = z(\tau), \quad \tau = mt \tag{4}$$

where $z(\tau)$ denotes the system response after scaling, τ is the time variable after scaling, and m is the scale coefficient. Then, equation (4) is substituted into (3)

$$\begin{cases} \frac{\mathrm{d}z}{\mathrm{d}\tau} = \frac{-a}{m}b\sin(bz) + \frac{1}{m}N\left(\frac{\tau}{m}\right) \\ N\left(\frac{\tau}{m}\right) = \sqrt{2Dm}\xi(\tau) \end{cases} \tag{5}$$

where $\xi(\tau)$ denotes Gaussian white noise with a mean value of 0 and a variance of 1. After sorting out, equation (5) can be expressed as

$$\begin{cases} \frac{\mathrm{d}z}{\mathrm{d}\tau} = \frac{-a}{m}b\sin(bz) + \sqrt{2Dm}\xi(\tau) \\ \langle \xi(\tau)\rangle = 0, \langle \xi(\tau), \xi(0)\rangle = \delta(\tau) \end{cases}. \tag{6}$$

Further, letting $\frac{a}{m} = a_1$, $b = b_1$, $Dm = D_1$, then equation (6) can be expressed as

$$\begin{cases} \frac{\mathrm{d}z}{\mathrm{d}\tau} = -a_1 b_1 \sin(b_1 z) + \sqrt{2D_1}\xi(\tau) \\ \langle \xi(\tau)\rangle = 0, \langle \xi(\tau), \xi(0)\rangle = \delta(\tau) \end{cases} \tag{7}$$

where a_1 and b_1 are the system parameters of the periodic potential system after general scale transformation. When m is a large enough constant, equations (7) and (3) have the same dynamic properties. Equation (7) is a general scale transformation CR model, according to which a weak signal with high frequency can be detected.

It can be seen that CR can be realized by adjusting system parameters a, b or noise intensity D. However, it is worth noting that the existing noise reduction methods may weaken the useful characteristic information. Thus, we only consider CR with parameter adjustment. At the same time, for the collected discrete signal, the fourth order Runge–Kutta algorithm [31] is used to solve the above equation and calculate the system output, as shown in equation (8)

$$\begin{cases} x_{i+1} = x_i + \frac{1}{6}\left(k_1 + 2k_2 + 2k_3 + k_4\right); \\ k_1 = h\left[-m^2 a_1 b_1 \sin\left(m b_1 x_i\right) + m N_i\right]; \\ k_2 = h\left\{-m^2 a_1 b_1 \sin\left[m b_1\left(x_i + \frac{1}{2}k_1\right)\right] + m N_i\right\}; \\ k_3 = h\left\{-m^2 a_1 b_1 \sin\left[m b_1\left(x_i + \frac{1}{2}k_2\right)\right] + m N_{i+1}\right\}; \\ k_4 = h\left\{-m^2 a_1 b_1 \sin\left[m b_1\left(x_i + k_3\right)\right] + m N_{i+1}\right\}; \end{cases} \tag{8}$$

where N_i denotes the discrete series of the input noise, x_i denotes the output series of the system, and h is the time step.

Meanwhile, considering the calculation speed and the optimal system output, quantum particle swarm optimization (QPSO) [32, 33] is used to find the optimal system parameters adaptively, improve the operation efficiency and obtain the optimal system output. We use SNR [34] as the fitness function of the optimization algorithm. Figure 1 shows the flow chart of adaptive CR using the QPSO algorithm. Usually, CR occurs at the Hopf bifurcation in former works [35, 36]. However, by the optimal algorithm, CR can occur at more frequencies but not only near the Hopf bifurcation.

2.2. Evaluation index

The performance of CR is influenced by both the noise and the nonlinear system. By introducing noise, the system output presents coherent oscillation. When the coherence appears, there is an obvious resonance band in the spectrum, and a great number of frequency components in the resonance band have large spectrum value. For SR, due to the existence of periodic input, the output presents synchronization with the input and there is only one high spectrum line but there is no resonance band. In order to describe the cooperative behavior between the noise and system in CR phenomenon further, we use the autocorrelation function to observe the periodic property of the output. The autocorrelation is defined by [26]

$$C_{xx}(\tau) = \langle \tilde{x}(t)\tilde{x}(t+\tau)\rangle / \left\langle \tilde{x}(t)^2 \right\rangle \tag{9}$$

where $\tilde{x}(t) = x(t) - \langle x(t)\rangle$, $\langle\cdot\rangle$ denotes the long-term average of the system, and $x(t)$ is the output of the system.

The SNR is another index to evaluate the CR output. In the diagnosis of bearing faults, we assume that the existing fault characteristic frequencies are the theoretical fault characteristic frequencies of the outer raceway, inner raceway and rolling element, respectively. Resonance optimization is performed at these imaginary fault characteristic frequencies. If the output is SR, the imaginary fault frequency exists. If the output is CR, the imaginary fault frequency does not exist. Its definition is

$$\mathrm{SNR} = 10\lg\frac{S(f)}{N(f)} \tag{10}$$

where $S(f)$ is the power of the output at the imaginary frequency in the spectrum. $N(f)$ is the average noise power near the imaginary frequency. The spectrum is obtained by the discrete output of the fast Fourier transform (FFT) calculation system. Specifically, $S(f)$ and $N(f)$ are calculated by

$$\begin{cases} S(f) = |X(k)|^2 \\ N(f) = \frac{1}{2M}\sum_{j=1}^{M}\left(|X(k-j)|^2 + |X(k+j)|^2\right) \end{cases} \tag{11}$$

where k is the spectrum serial number corresponding to the input signal frequency, $X(k)$ is the amplitude of the input frequency, M is determined according to the sampling point and sampling frequency. It is noted that the SNR is performed at the assumed fault characteristic frequency because the influence of load is not considered when calculating the theoretical fault characteristic frequency. For the actual fault characteristic frequency, there is little difference between the actual fault characteristic frequency and the theoretical fault characteristic frequency. According to our previous research results [37], it is also feasible to calculate the SNR at the actual fault characteristic frequency by using the theoretical fault characteristic frequency.

Considering that only by observing the autocorrelation function and spectrum of the output of the system, the result of the distinction is not convincing and cannot meet the accuracy requirement of bearing fault detection. We need a much more intuitive way of judging, not just by comparing the frequency spectrum. Hu *et al* introduced the quality factor index to describe the CR phenomenon of the system [21]. Here we define the resonance factor in the response spectrum to quantify the CR degree,

$$\beta = A(f)/A_s. \tag{12}$$

$A(f)$ denotes the magnitude of the imaginary frequency in the response spectrum, and A_s denotes the sum of all amplitudes more than $A(f)/2$ in the response spectrum. CR is a cooperative behavior of the noise and the non-linear system. When CR occurs, due to the existence of the spectral resonance band, there are a large number of interference frequencies near the imaginary frequency in the response spectrum. When SR occurs, there is little interference frequency, and the value of resonance factors will approach 1. However, when CR occurs, the index is much smaller. When the resonance factor changes from a small value to a much larger value, the CR will transform to SR. By calculating the response spectrum resonance factor, we can judge whether CR or SR occurs to accurately evaluate the bearing state.

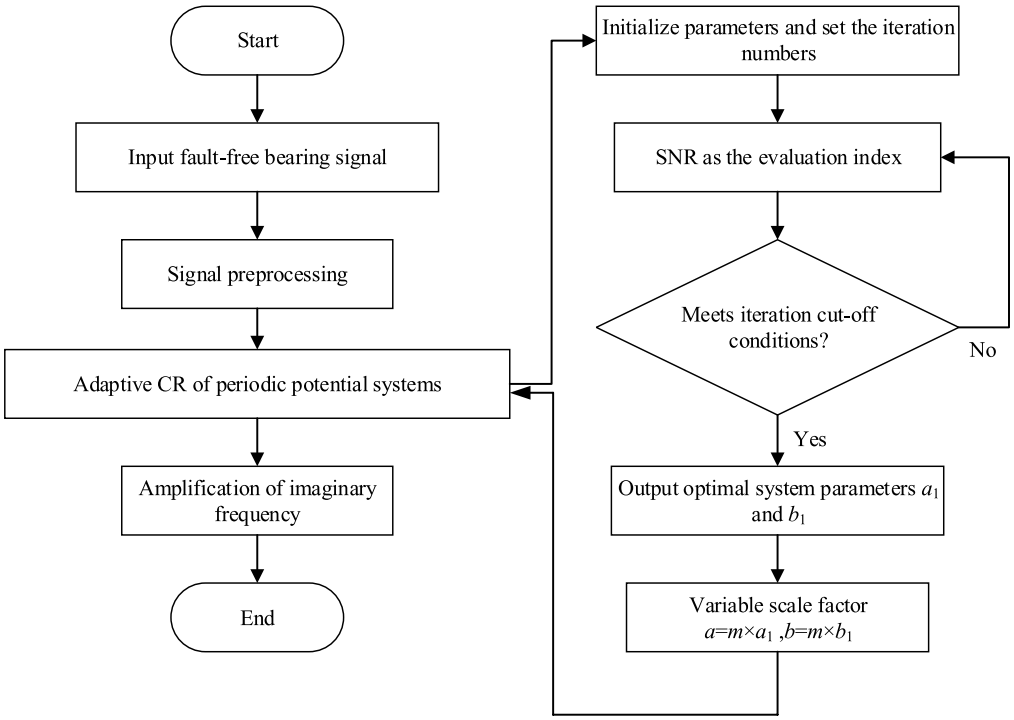

Figure 1. Flowchart of adaptive CR.

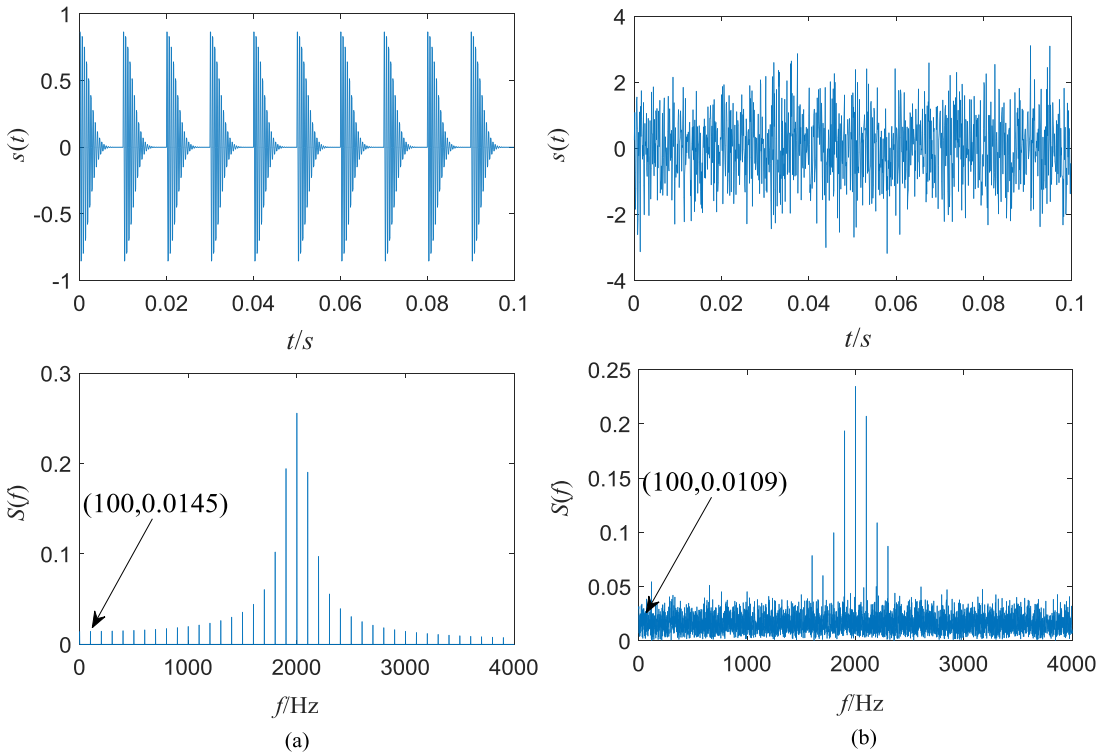

Figure 2. Time-domain waveform and frequency spectrum of the simulation input signal. (a) Without noise; (b) with noise.

3. Numerical simulation

In order to intuitively illustrate the existence of CR phenomenon and explore the effectiveness of the above method in bearing fault detection, the simulation bearing vibration signal with an outer raceway fault at frequency $f = 100$ Hz is selected as the driving force. The bearing vibration signals with other faults are no longer described here, but we will analyze them in the experimental verification. The bearing vibration signal with an outer raceway fault contains a series of attenuation pulses [38], which are generated by the formula

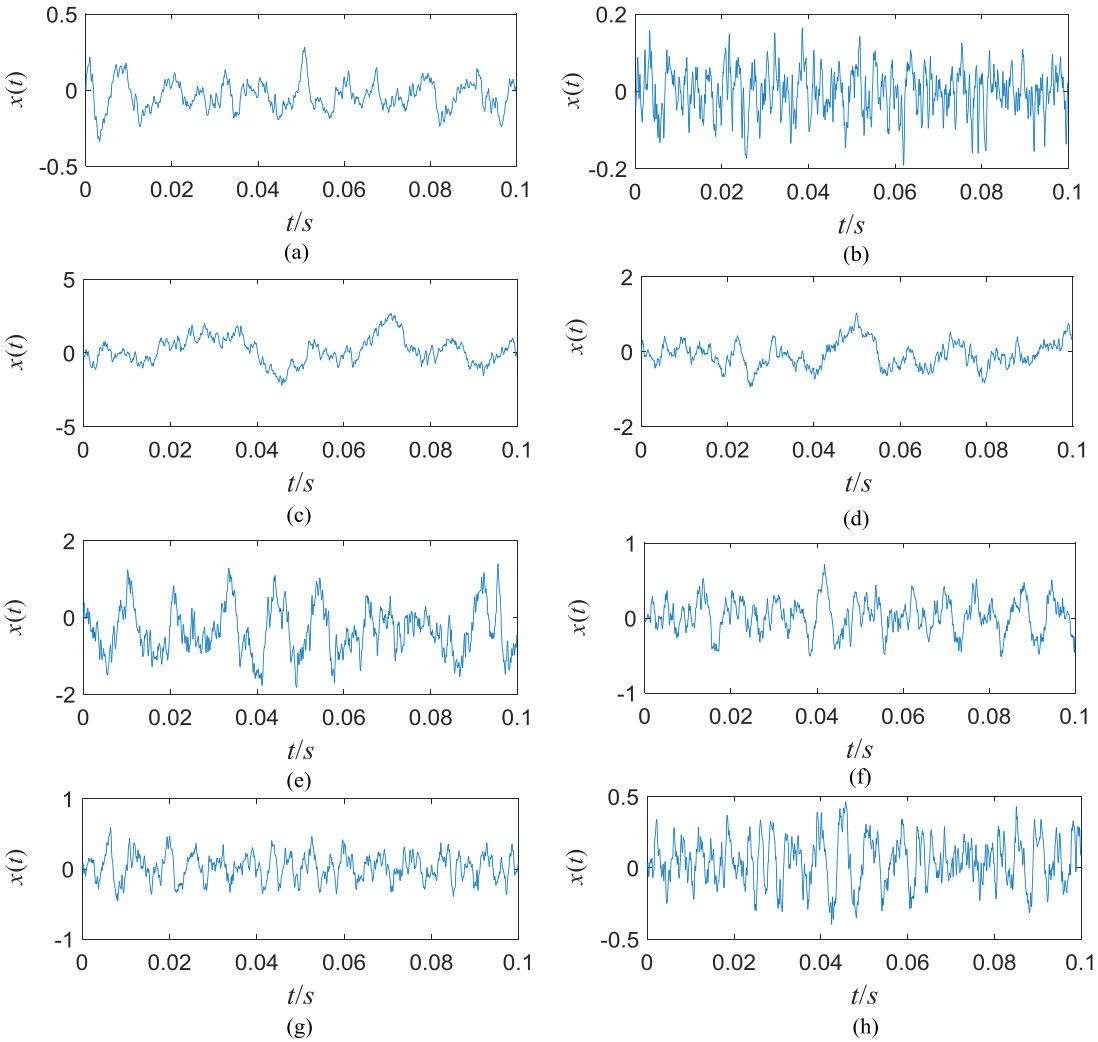

Figure 3. System output time-domain waveform. (a) The SR output corresponding to $f = 100$ Hz; (b)–(h) the CR output corresponding to $f = 100$ Hz, $f = 30$ Hz, $f = 50$ Hz, $f = 80$ Hz, $f = 130$ Hz, $f = 150$ Hz and $f = 180$ Hz respectively.

$$\begin{cases} s(t) = A\sin(2\pi f_n t) \times \exp\left\{-B[t - r(t)/f_d]^2\right\} \\ r(t) = t \times f_d \end{cases} \tag{13}$$

where A is the amplitude of the pulse signal, B is the attenuation coefficient, and f_n and f_d are natural frequency and fault frequency respectively. $r(t)$ is the number of repetitions. In this simulation, the specific parameters are set as follows: sampling frequency $f_s = 12\,000$ Hz, sampling point $n = 12\,000$, signal amplitude $A = 1$, natural frequency $f_n = 2000$ Hz, fault frequency $f_d = 100$ Hz, attenuation coefficient $B = 120\,000$, repetition number $r(t) = 10$. Figures 2(a) and (b) shows the original signal and the noisy simulation signal, respectively.

As shown in figure 2, the modulation frequency of the original noisy signal is visible, but the fault frequency is completely submerged by the noise. Therefore, in order to eliminate interference and obtain more useful information, it is decided to pre-process the modulated simulation signal [39, 40]. Hilbert transform is used to de-modulate the signal, extract the fault features, and high-pass filter the demodulated signal to get the envelope signal. Next, in order to illustrate the universal existence of CR, the resonance output of the original simulated signal periodic potential system with noise and the CR output at different imaginary frequencies with signal amplitude $A = 0$ are obtained respectively.

As we mentioned before, for CR, there is no periodic signal in the input. However, for SR, there is a specific periodic signal in the excitation. To verify some discerptions above, figures 3 and 4 show the time-domain waveforms and frequency spectrum of the system output respectively. In order to illustrate the existence of CR in bearing fault diagnosis, and to analyze the difference with SR. We study the SR of bearing simulation signal with $f = 100$ Hz, and we also study CR at the imaginary frequencies $f = 30$ Hz, 50 Hz, 80 Hz, 100 Hz, 130 Hz, 150 Hz and 180 Hz respectively. As can be seen from figure 3, the waveforms in each time domain show a certain periodicity, but in figure 3(a) the periodic property is obviously strongest. Reflected in the frequency spectrum, the peak at the characteristic frequency in figure 4(a) are obviously higher than that of other frequencies, indicating that SR occurs. However, several noise components in the frequency spectrum, which are of the same magnitude as the characteristic frequency, cannot be ignored. It is worth noting that there are resonance bands in

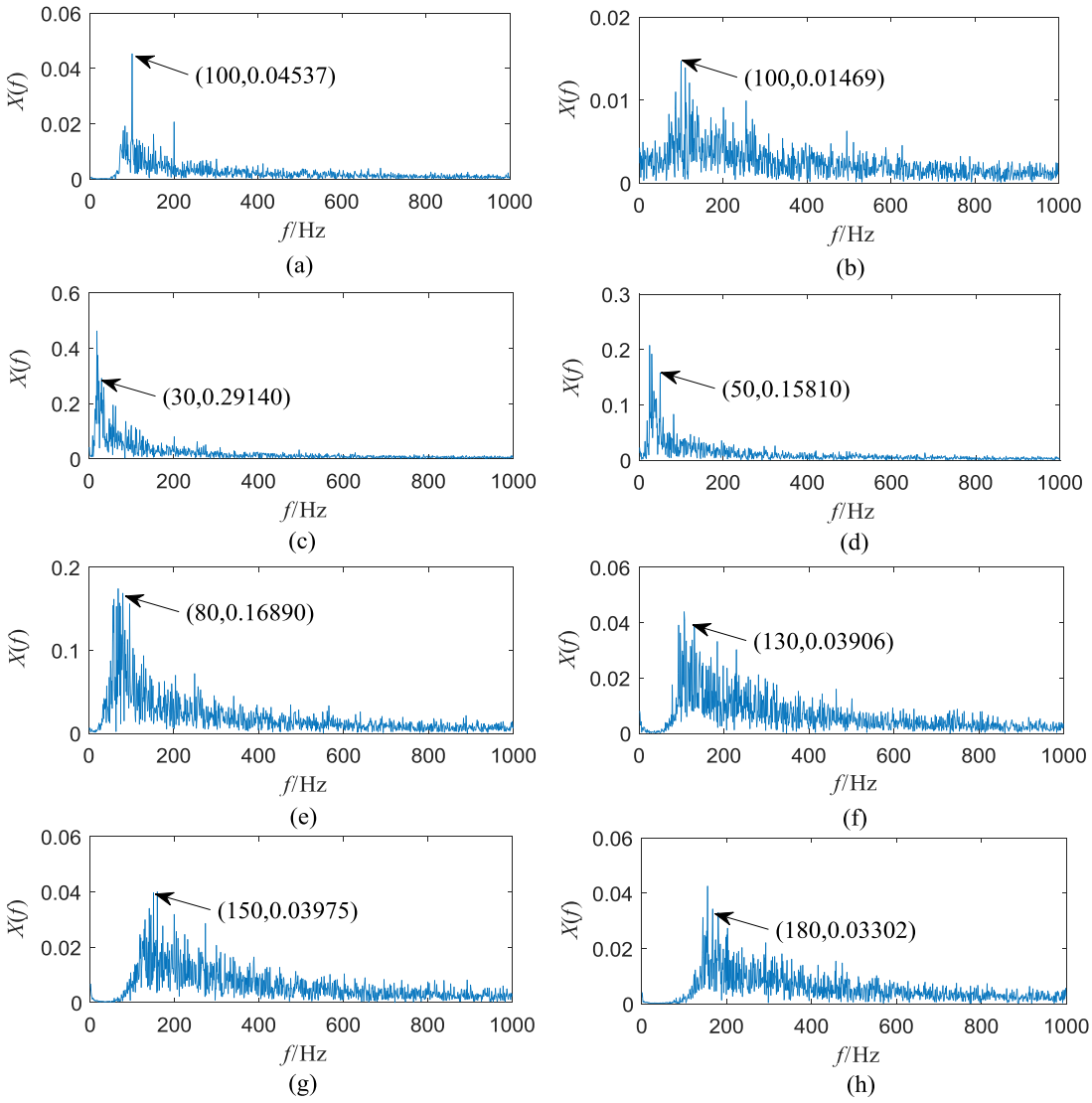

Figure 4. System output response frequency spectrum. (a) The SR output corresponding to $f = 100$ Hz; (b)–(h) the CR output corresponding to $f = 100$ Hz, $f = 30$ Hz, $f = 50$ Hz, $f = 80$ Hz, $f = 130$ Hz, $f = 150$ Hz and $f = 180$ Hz respectively.

the frequency spectrum in figures 4(b)–(h), and the imaginary frequency is also obvious, which shows that CR is common. At the same time, there are a large number of strong interference frequencies in the resonance band, which is consistent with the theoretical analysis results.

The output of the system shows that there are differences between CR and SR. Moreover, with the enhancement of the characteristic frequency, CR at the imaginary frequency shown in figure 4 will gradually convert to SR. However, as far as the above results are concerned, this conversion phenomenon is not obvious enough. In other words, judging by system output only is not convincing. We need to do further analysis and processing of resonance output. Therefore, we introduce the autocorrelation function to analyze the resonance output of the system. The results are given in figure 5.

From the definition of the autocorrelation function, the stronger the periodic oscillation of the autocorrelation function, the more obvious the periodic components in the time series will be. The autocorrelation function represented by figure 5 shows different degrees of periodic oscillation with increasing time, and the frequency of the oscillation is consistent with the imaginary frequency. Among them, the autocorrelation function of SR output in figure 5(a) has the most obvious oscillation and the strongest periodic component. The same result can be obtained from the frequency spectrum of the autocorrelation function in figure 6. Moreover, compared with the resonance output frequency spectrum in figure 4, the interference information in the frequency spectrum is greatly reduced, and the frequency component with the highest power in the spectrum just indicates the characteristic frequency. Then, the detection effect is obviously improved. Figures 6(b)–(h) shows the CR autocorrelation spectrum at different imaginary frequencies. Compared with the system resonance output, the high frequency noise is also suppressed, and the spectrum resonance band is more obvious. A large number of interference frequencies amplified synchronously with characteristic frequencies in the resonance band are the powerful manifestation of CR. The results show that the imaginary characteristic frequency generated by CR cannot provide evidence of structural defects in bearings.

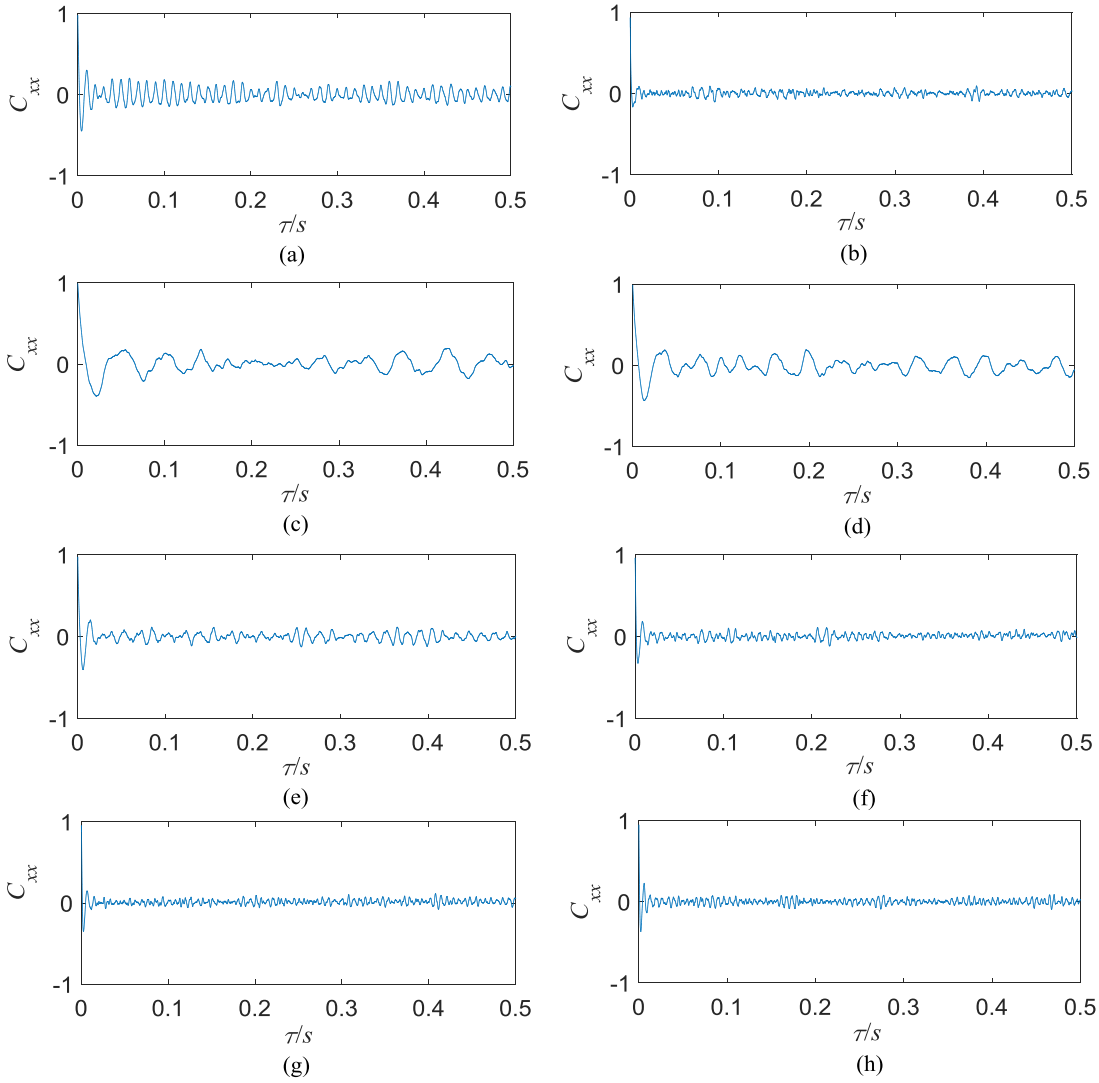

Figure 5. System output autocorrelation function. (a) The SR output corresponding to $f = 100$ Hz; (b)–(h) the CR output corresponding to $f = 100$ Hz, $f = 30$ Hz, $f = 50$ Hz, $f = 80$ Hz, $f = 130$ Hz, $f = 150$ Hz and $f = 180$ Hz respectively.

Therefore, by calculating the autocorrelation function of the resonance output of the system, we have basically realized the diagnosis of fault features. However, the above methods are still carried out under the condition of comparison. For bearing signals whose pre-condition is completely unknown, we lack the basis of intuitive judgment. Therefore, we propose a resonance factor index to quantify the results without comparing the spectrum structure. The transition from CR to SR can be separated from the numerical value, and the weak periodic signal can be judged. By calculating the resonance factor of each spectrum in figure 6, the values are 1, 0.5585, 0.1253, 0.2059, 0.1234, 0.0846, 0.2387 and 0.1747, respectively. It illustrates that the resonance factor index is effective in measuring the CR phenomenon and evaluation of bearing faults.

4. Experimental verification

The effectiveness of the proposed method is proved by the analysis of the above simulation signals. We also hope the new method is effective in processing the signal obtained from the experimental platform. In this section, we will use several sets of experimental signals to verify the validity of this method in bearing fault evaluation.

4.1. Bearing data from experimental platform

Based on the results of numerical simulation, the robustness of the novel bearing fault detection method proposed in this paper is further verified. Therefore, we use the experimental data collected from the experimental platform to detect and analyze the bearing fault and illustrates the advantages of the periodic potential system through experiments. Bearing data is collected from our experimental platform. The layout of the experimental platform is shown in figure 7.

As shown in the figure, the frequency inverter under the platform is used to control the Y2VF 90L 4-B3 motor and output invariable rotating velocities. A radial loading device and magnetic powder brake provide radial force and brake torque respectively. The specific values of radial loading force and torque can be read from an FZ-A-100 dynamometer and

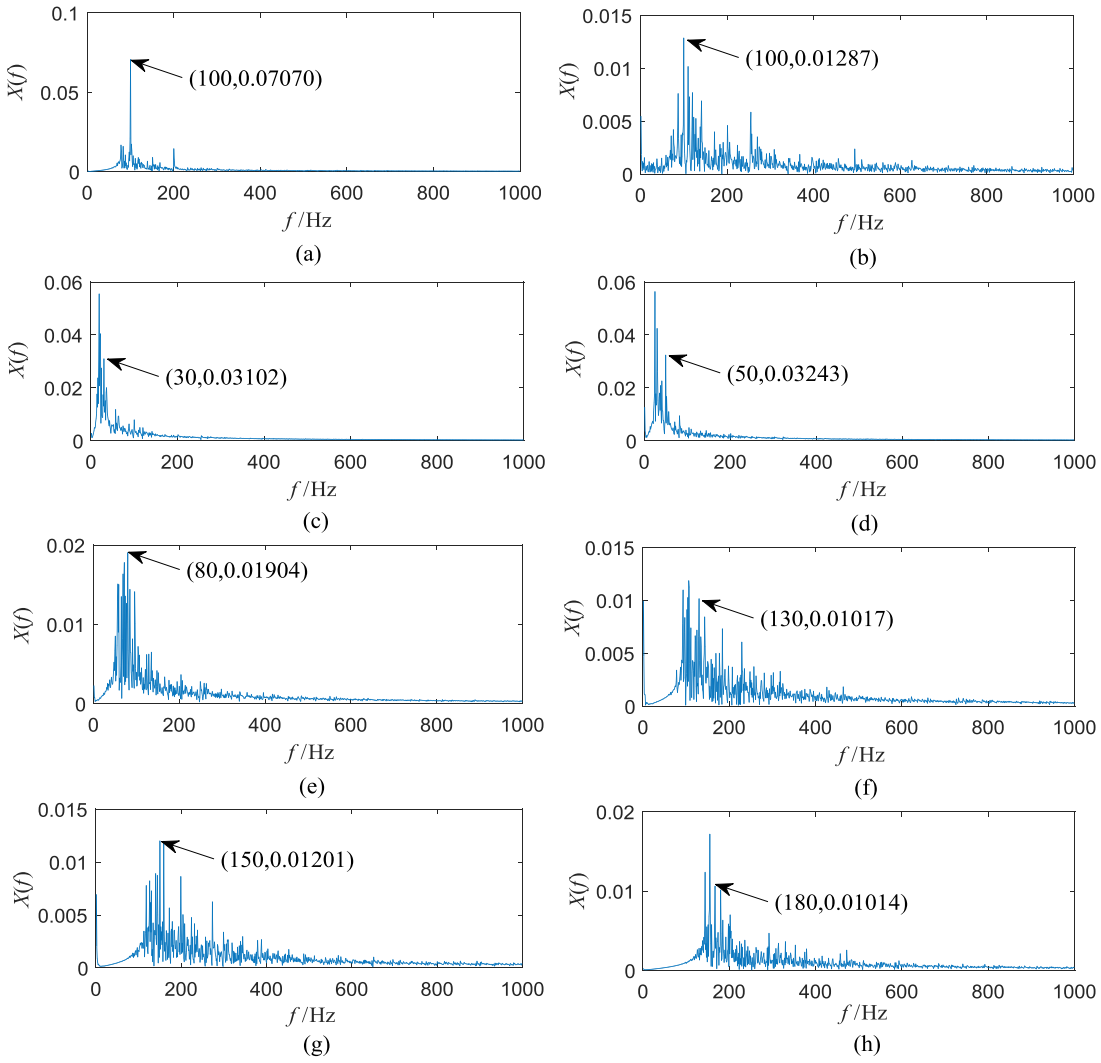

Figure 6. System output autocorrelation function frequency spectrum. (a) The SR output corresponding to $f = 100$ Hz; (b)–(h) the CR output corresponding to $f = 100$ Hz, $f = 30$ Hz, $f = 50$ Hz, $f = 80$ Hz, $f = 130$ Hz, $f = 150$ Hz and $f = 180$ Hz respectively.

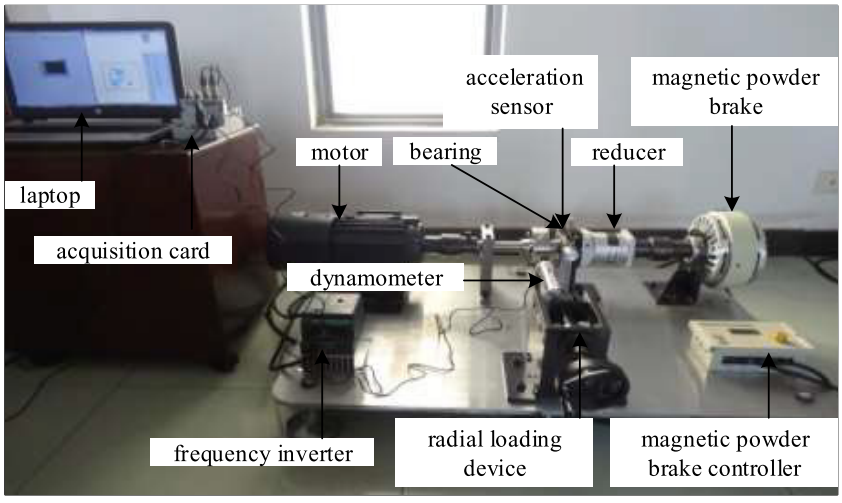

Figure 7. Experimental platform.

ZL2A-5S magnetic particle brake controller respectively. The vibration data collected by the acceleration sensor installed on the bearing seat is transmitted to the laptop through the acquisition card for data analysis and processing. The types of acceleration sensor and acquisition card are 1A206E and NI9234. The types of the tested cylindrical roller bearings are NU306E and N306E. The pitting faults of the outer raceway, inner raceway and rolling element are processed

Table 1. Experimental bearing data.

	Fault type	Bearing type	Rotating speed	Outer raceway fault frequency	Inner raceway fault frequency	Rolling element fault frequency
1	Outer raceway fault	N306E	1423 rpm	105.35 Hz		
2	Inner raceway fault	NU306E	1427 rpm		172.08 Hz	
3	Rolling element fault	N306E	1427 rpm			119.01 Hz
4	Normal bearing	N306E	1431 rpm	105.94 Hz	156.40 Hz	119.41 Hz

Table 2. The structural parameters of the cylindrical roller bearing.

Outer raceway diameter	Inner raceway diameter	Pitch diameter	Rolling element diameter	Thickness	Number of rolling elements
72 mm	30 mm	51 mm	10.5 mm	19 mm	12

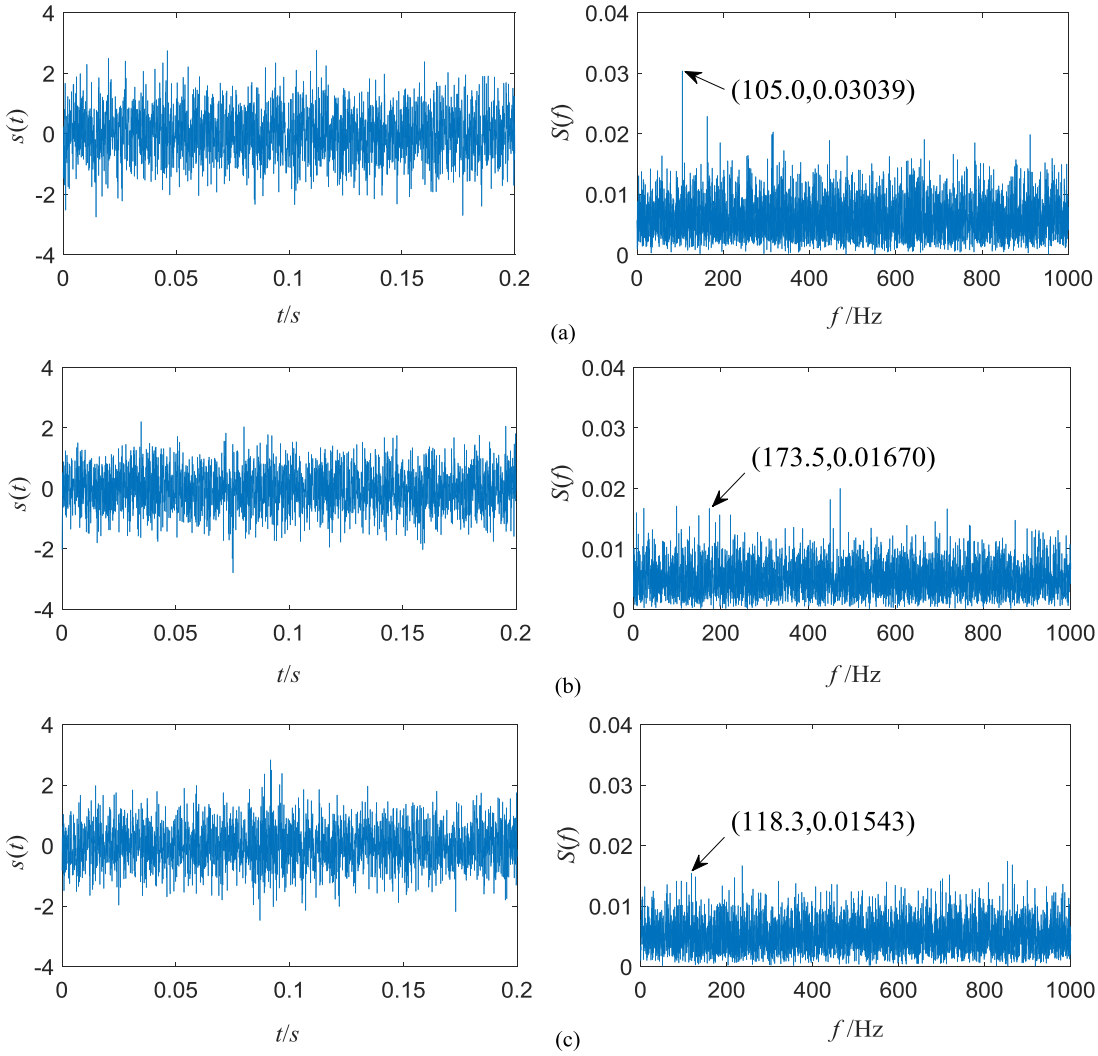

Figure 8. Time-domain waveform and frequency spectrum of the raw bearing fault experimental signal. (a) Outer raceway fault; (b) inner raceway fault; (c) rolling element fault.

respectively for different types of bearings. The size of the fault is 0.5 mm × 1.2 mm (depth × width). In the experiment, the cylindrical roller bearings with different fault types and normal conditions were tested on the above experimental platform. The actual rotational speeds of three kinds of fault bearings and normal bearings are measured, and the theoretical fault frequencies of normal bearings and the fault frequencies of bearings with different fault types are calculated. Specific bearing type, actual speed and fault frequency are shown in table 1. Test bearing structure parameters are shown in table 2. Sampling frequency $f_s = 12\,800$ Hz and sampling point $n = 51\,200$.

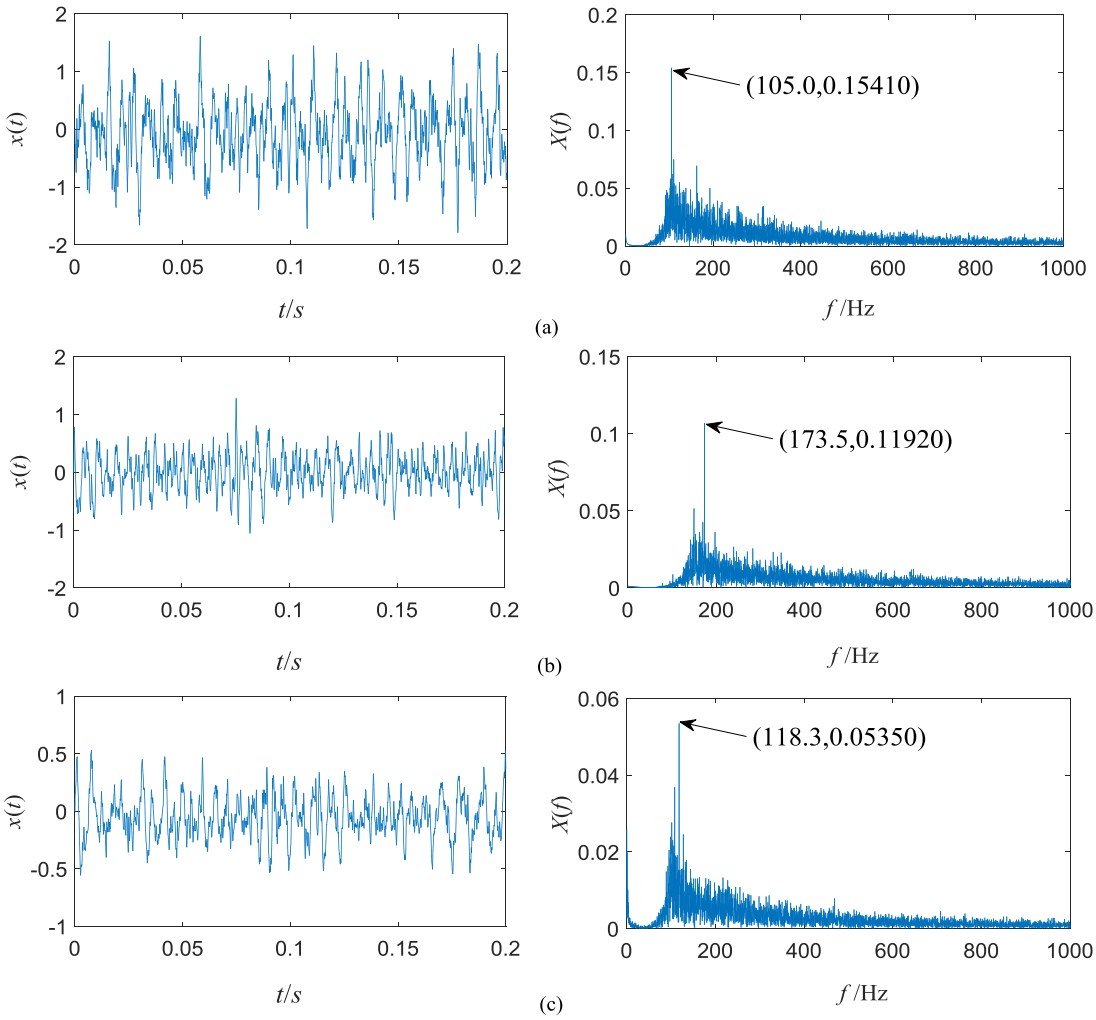

Figure 9. SR output time domain waveform and frequency spectrum. (a) Outer raceway fault; (b) inner raceway fault; (c) rolling element fault.

4.2. Analysis of fault bearing signal by proposed method

In order to verify the applicability of the proposed method for fault diagnosis of actual bearings, we have carried out the same treatment process for three different fault bearings and normal bearings. It is hoped that the bearing faults can be evaluated by the difference of resonance factor values.

Firstly, three sets of bearing signals with an outer raceway, inner raceway and rolling element faults are acquired. The time domain waveform and frequency spectrum of the original signal are shown in figure 8. As can be seen, the impulse component of the fault is completely submerged by strong noise, and the original signal cannot provide any effective information for bearing fault detection. Therefore, we use the adaptive method to find the best system parameters and get the system resonance output of the envelope signal, which is obtained by demodulating and filtering the original signal.

Figure 9 presents the SR output of three sets of faults bearing signals. It can be seen from the time domain waveform that there are periodic fault pulses. Different fault types in the spectrum are identified and extracted. The amplitude of the characteristic frequency line is enhanced, but the noise energy in the high frequency region is not fully converted to the characteristic frequency. Although the fault can be detected, the accidentally amplified noise component around the characteristic frequency may cause problems in the detection results. In order to improve the accuracy of fault detection, the output of the system is analyzed by the autocorrelation function.

As shown in figure 10, the waveforms of the output autocorrelation function show strong periodic oscillation, and the oscillation frequency is the same as the fault frequency, showing the fault characteristics to the greatest extent. At the same time, figures 10(a)–(c) shows the frequency spectrum of the autocorrelation function of the outer raceway, inner raceway and rolling element fault system respectively. Compared with figure 9, the line of fault characteristic frequency is more prominent, and there are no other interference frequency components around it. Comparing figure 9(a) with 10(a), it is not difficult to find that the amplitude of noise around the characteristic frequency 105 Hz in figure 9(a) is generally maintained at about 0.05, which is about one third of the amplitude at the characteristic frequency. In figure 10(a), amplitudes of these noises are generally maintained at about 0.02, which is about one tenth of the amplitudes at the characteristic frequency. The noise energy in

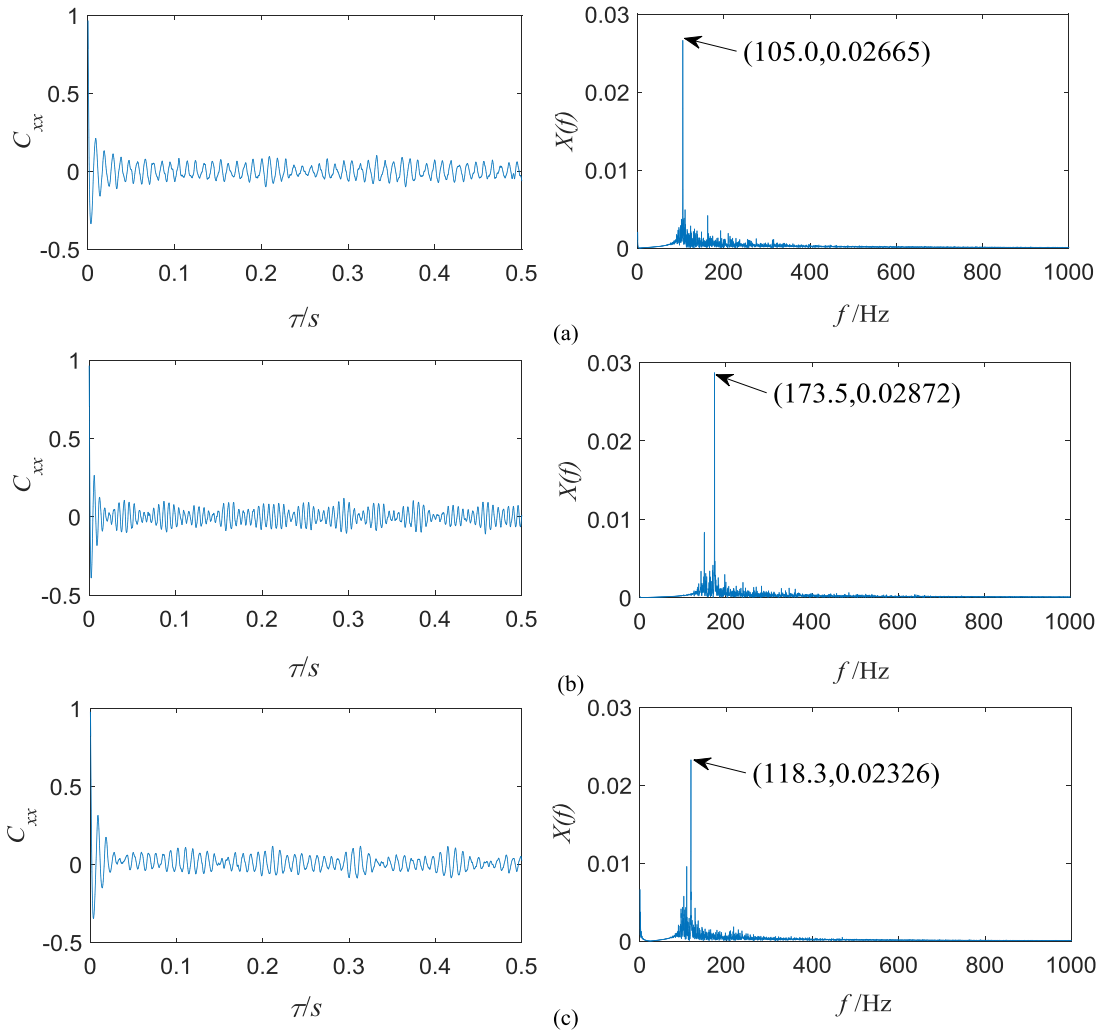

Figure 10. SR output autocorrelation function time domain waveform and frequency spectrum. (a) Outer raceway fault; (b) inner raceway fault; (c) rolling element fault.

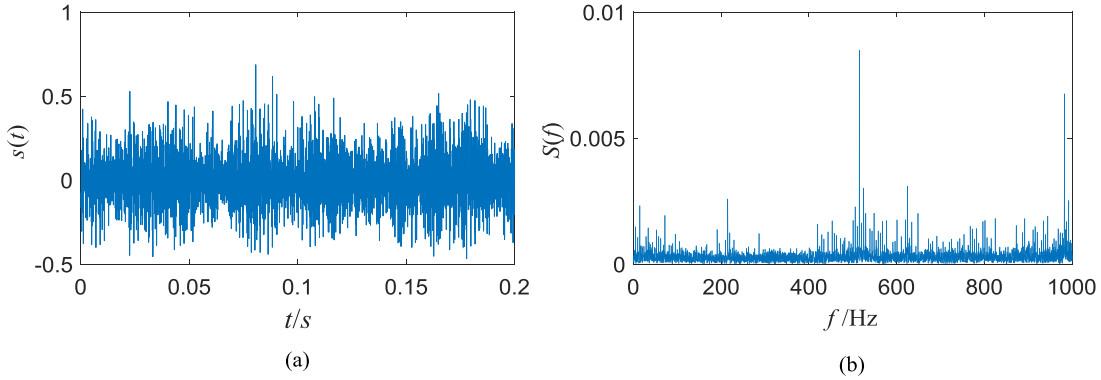

Figure 11. The raw normal bearing experimental signal. (a) Time domain waveform; (b) frequency spectrum.

the high frequency region is more fully transformed to the characteristic frequency, and the ability of utilizing noise is greatly enhanced. It is more advantageous to identify fault features. The resonance factor index of each frequency spectrum of figures 10(a)–(c) is calculated, and all values equal 1. From the simulation signal analysis results, it is not difficult to conclude that CR is transformed into SR because of the weak characteristic information of the bearing vibration signal. Thus, distinguishing SR and CR can accurately identify the bearing state.

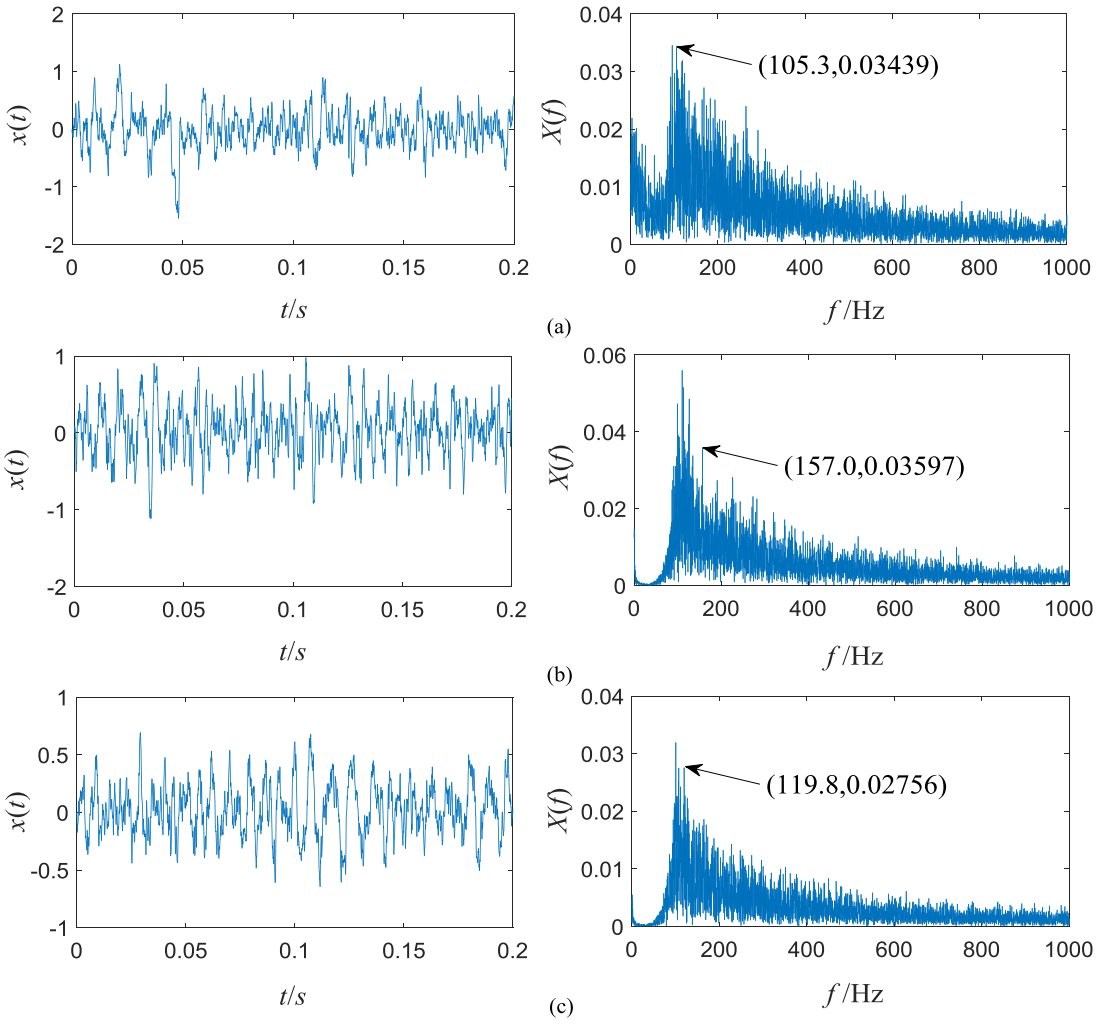

Figure 12. The adaptive CR output time-domain waveform and spectrum at theoretical fault frequencies. (a) Outer raceway fault; (b) inner raceway fault; (c) rolling element fault.

4.3. Analysis of normal bearing signal by the proposed method

In this part, we illustrate the importance of CR by analyzing the normal bearing signal and the effectiveness of a novel method based on CR in evaluating bearing faults. Figure 11 is the time domain waveform and the corresponding frequency spectrum of the normal bearing signal. It can be seen that there is no obvious fault pulse in the time domain waveform, and the characteristic frequency cannot be observed in the spectrum. Therefore, we also preprocess the normal signal to get the envelope signal after demodulation and filtering. We let the theoretical fault frequencies of the outer raceway, inner raceway and rolling element as the target frequency respectively, and the output results of the system are observed in figure 12.

Figure 12 shows the system output of normal bearing vibration signal after adaptive CR optimization. In figures 12(a)–(c) that when there is no fault, the fault characteristic line can also be obtained from the system output optimized by the optimization algorithm, and the high frequency noise energy is also converted to energy at the target frequency. This brings inconvenience to fault detection, and further proves the universality of the phenomenon of CR and its importance in bearing fault evaluation. Next, we analyze the autocorrelation function of figure 12 to observe the periodicity of the system output and further improve the observable quality of the frequency spectrum.

The results of autocorrelation function analysis are shown in figure 13. In figures 13(a)–(c) respectively represents the autocorrelation function of the system output after optimizing the theoretical fault frequency of the outer raceway, inner raceway and rolling element of the normal bearing test signal. It is worth noting that, like fault bearings, the conversion of high frequency noise energy to fault characteristic frequency is more obvious than the output of the system directly optimized, which is more conducive to analysis. Further analysis shows that the occurrence of CR can also lead to the extraction of fault features from normal bearing experimental signals, but by comparing figure 10 with 13, the oscillation amplitude of the autocorrelation function in figure 13(a) is significantly smaller than that of figure 10(a), and the oscillation frequency cannot keep synchronization with the fault frequency. The spectrum information of figure 13(a) is more complex than that of figure 10(a), the former containing more interference frequencies and has obvious resonance bands. Most of the

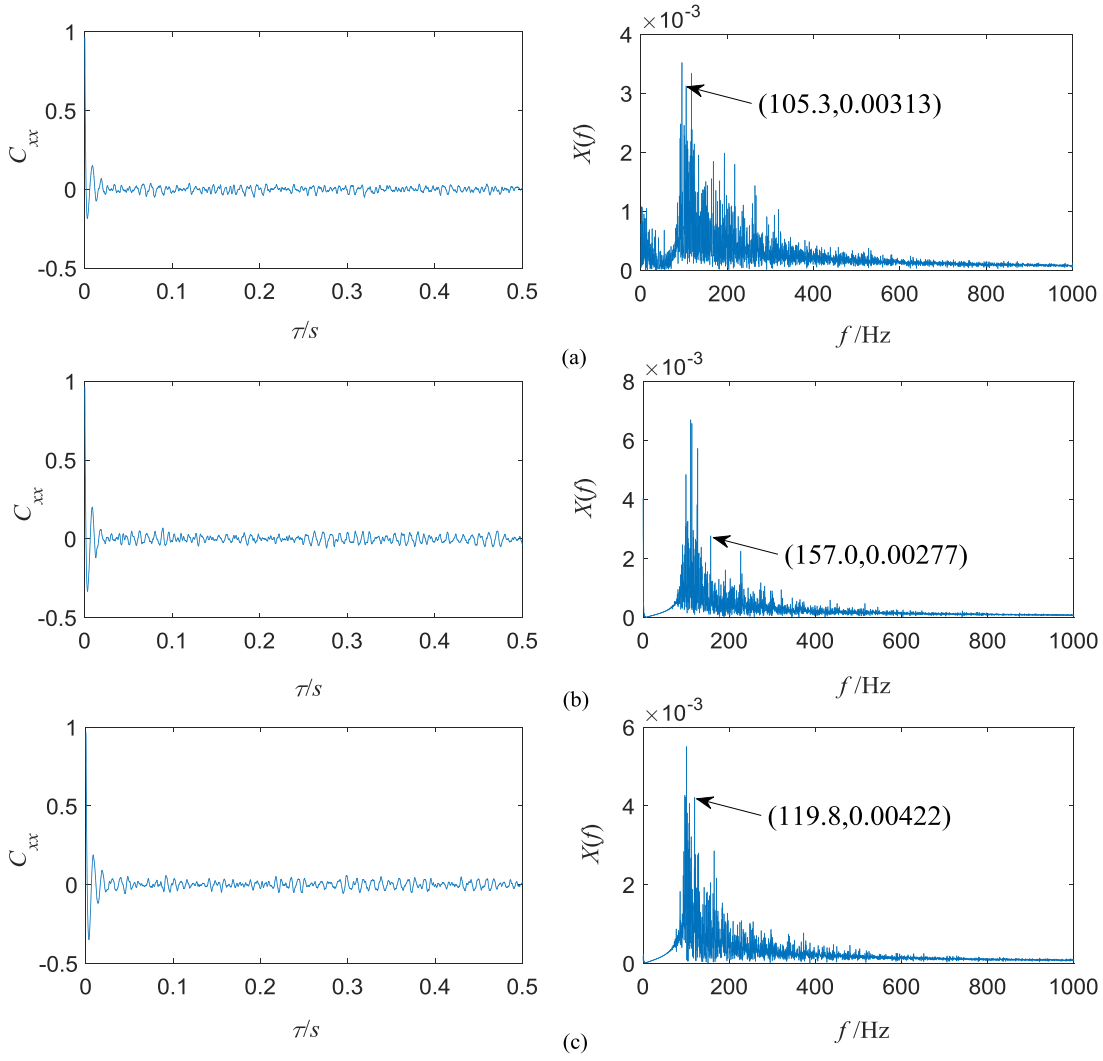

Figure 13. The adaptive CR output autocorrelation function time-domain waveform and spectrum at theoretical fault frequencies. (a) Outer raceway fault; (b) inner raceway fault; (c) rolling element fault.

noise components are not well suppressed. The resonance factors of figure 13 are calculated to be 0.1169, 0.0249 and 0.0852, respectively. All of them are close to 0, far less than the resonance factor index 1 of the output autocorrelation frequency spectrum of the fault bearing. It is worth noting that the increase of resonance factor index (from 0 to 1) corresponds to the transition from CR to SR, and the rolling bearing state also changes from normal to fault. Therefore, this index has a good effect on evaluating bearing faults.

It can be seen that the method in this paper has a good performance on both simulation and experiment signals and has sufficient robustness to detect bearing fault features, which is of great significance in bearing fault evaluation.

4.4. System model comparison

We validate the effectiveness of the new method based on the periodic potential system. Next, we use a set of experimental signals to explain why we choose the periodic potential instead of the classical bistable potential with potential $U(x) = -\frac{a}{2}x^2 + \frac{b}{4}x^4$.

The former works show that periodic potential systems are easy to match different input signals [26]. For a periodic potential system, changing parameters a or b can only change the depth or width of potential wells. However, for a bistable system, changing a system parameter will lead to simultaneous changes in the width and depth of the potential well, which brings inconvenience to parameter optimization. Figures 14(a) and (b) show the process of parameter optimization of the periodic potential system and bistable system respectively. When the periodic potential system reaches the optimum, the number of iterations is 4, the calculation time is 55.69 s, the improved SNR is 2.445 dB, and the number of iterations is 25 times when the bistable system reaches the optimum, the time of optimization is 139.65 s, and the improved SNR is 0.336 dB. It can be seen that when CR occurs, the number of iterations of the periodic potential system is much less than that of the bistable system, the time of optimization is shortened by

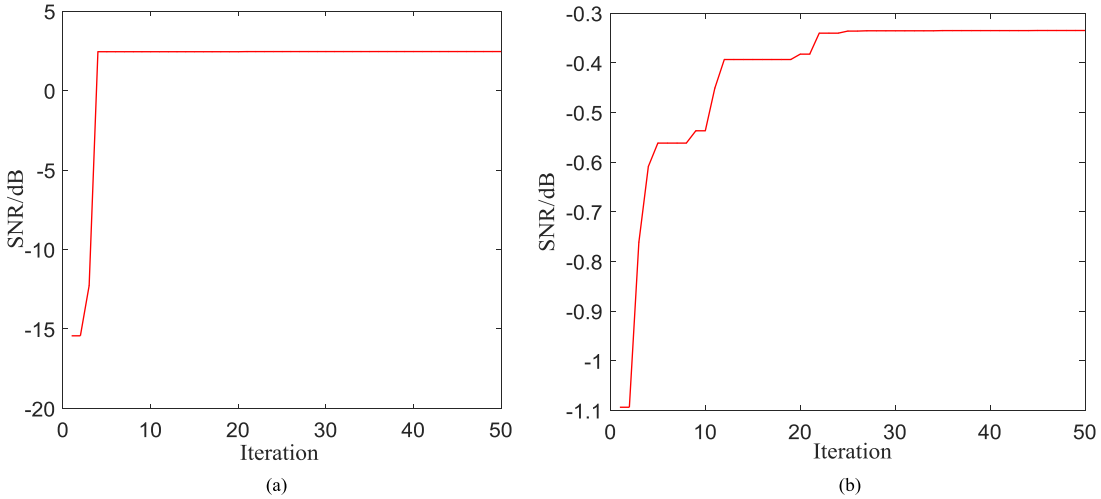

Figure 14. Iterative curve at the theoretical fault frequency of the inner raceway of the normal bearing signal: (a) periodic potential system (calculation time: 55.69 s); (b) bistable system (calculation time: 139.65 s).

more than half, and the improved SNR is obviously improved. In summary, the periodic potential system has more advantages than the bistable system in reducing the number of iterations, saving the calculation time and improving the SNR in CR.

5. Conclusion

In former works of bearing fault diagnosis by the SR method, the actual characteristic frequency should be known in prior. It limits the application of the method. In fact, if we give a wrong characteristic frequency, the resonance named CR, which is very similar to SR, will also occur. If we do not distinguish SR and CR, we will misjudge the health state of the bearing.

In this paper, a method of bearing fault detection based on CR is proposed, which overcomes the problem that it is impossible to determine the existing characteristic signal only by using SR for bearing fault diagnosis. The existence of CR and the importance of bearing fault detection are proved by the system output of normal simulation signal at different frequencies. The output of the system is further analyzed by introducing the autocorrelation function. By comparing the waveform and spectrum structure of the autocorrelation function, the measurement of CR is successfully realized, which shows that CR can convert to SR. The resonance factor index is constructed to quantify the analysis results without comparison, and the bearing fault detection is realized. The advantages of the periodic potential system over the bistable system in computing speed and improving SNR are analyzed. The effectiveness and applicability of the proposed method in bearing fault evaluation are verified by numerical simulation and experiment. Due to the limitation of the length of the paper, we only give a primer exploration in CR in bearing fault evaluation. We stress whether the bearing state is in health or in failure. However, the severity degree is not discussed. In the following work, based on the measurement of CR, we will design a new experiment to solve the problem. Moreover, we think the method in this paper can also be used in the evaluation of the health of other components of rotating machinery.

Acknowledgments

The project was supported by the National Natural Science Foundation of China (Grant No.11672325), the Key Project of National Natural Science Foundation of China (Grant No. U1510205), the joint Fund of the Ministry of Education of China (6141A020331), the Priority Academic Program Development of Jiangsu Higher Education Institutions and the Top-notch Academic Programs Project of Jiangsu Higher Education Institutions.

ORCID iDs

Jianhua Yang https://orcid.org/0000-0001-5389-9142

References

[1] Lu W, Jiang W, Wu H and Hou J 2012 A fault diagnosis scheme of rolling element bearing based on near-field acoustic holography and gray level cooccurrence matrix *J. Sound Vib.* **331** 3663–74
[2] Lin J and Qu L 2000 Feature extraction based on Morlet wavelet and its application for mechanical fault diagnosis *J. Sound Vib.* **234** 135–48
[3] Bin G, Gao J, Lin X and Dhillon B S 2012 Early fault diagnosis of rotating machinery based on wavelet packets—empirical mode decomposition feature extraction and neural network *Mech. Syst. Signal Process.* **27** 696–711
[4] He W, Zi Y, Chen B, Wu F and He Z 2015 Automatic fault feature extraction of mechanical anomaly on induction motor bearing using ensemble super-wavelet transform *Mech. Syst. Signal Process.* **54** 457–80
[5] Zhang S, Wang Y, He S and Jiang Z 2016 Bearing fault diagnosis based on variational mode decomposition and total variation denoising *Meas. Sci. Technol.* **27** 075101
[6] Cheng G, Chen X, Li H, Li P and Liu H 2016 Study on planetary gear fault diagnosis based on entropy feature

fusion of ensemble empirical mode decomposition *Measurement* **91** 140–54
[7] Yan R, Gao R X and Chen X 2014 Wavelets for fault diagnosis of rotary machines: a review with applications *Signal Process.* **96** 1–15
[8] Widodo A and Yang B 2007 Support vector machine in machine condition monitoring and fault diagnosis *Mech. Syst. Signal Process.* **21** 2560–74
[9] Yu Y, Yu D and Cheng J 2006 A roller bearing fault diagnosis method based on EMD energy entropy and ANN *J. Sound Vib.* **294** 269–77
[10] Lou X and Loparo K A 2004 Bearing fault diagnosis based on wavelet transform and fuzzy inference *Mech. Syst. Signal Process.* **18** 1077–95
[11] Lu S, He Q and Wang J 2019 A review of stochastic resonance in rotating machine fault detection *Mech. Syst. Signal Process.* **116** 230–60
[12] Benzi R, Sutera A and Vulpiani A 1981 The mechanism of stochastic resonance *J. Phys. A: Math. Gen.* **14** 453–7
[13] Hu B and Li B 2016 A new multiscale noise tuning stochastic resonance for enhanced fault diagnosis in wind turbine drivetrains *Meas. Sci. Technol.* **27** 025017
[14] Jiang K, Xu G, Liang L, Tao T and Gu F 2014 The recovery of weak impulsive signals based on stochastic resonance and moving least squares fitting *Sensors* **14** 13692–707
[15] Qiao Z, Lei Y and Li N 2019 Applications of stochastic resonance to machinery fault detection: a review and tutorial *Mech. Syst. Signal Process.* **122** 502–36
[16] Li J, Li M and Zhang J 2017 Rolling bearing fault diagnosis based on time-delayed feedback monostable stochastic resonance and adaptive minimum entropy deconvolution *J. Sound Vib.* **401** 139–51
[17] Lu S, He Q, Dao D and Kong F 2016 Periodic fault signal enhancement in rotating machine vibrations via stochastic resonance *J. Vib. Control* **22** 4227–46
[18] Xia P, Xu H, Lei M and Ma Z 2018 An improved stochastic resonance method with arbitrary stable-state matching in underdamped nonlinear systems with a periodic potential for incipient bearing fault diagnosis *Meas. Sci. Technol.* **29** 085002
[19] He Q, Wu E and Pan Y 2018 Multi-scale stochastic resonance spectrogram for fault diagnosis of rolling element bearings *J. Sound Vib.* **420** 174–84
[20] Li X and Zhao D 2017 Coherence resonance and stochastic bifurcation in standing-wave thermoacoustic systems *J. Acoust. Soc. Am.* **141** 3958
[21] Hu G, Ditzinger T, Ning C Z and Haken H 1993 Stochastic resonance without external periodic force *Phys. Rev. Lett.* **71** 807
[22] Giacomelli G, Giudici M, Balle S and Tredicce J R 2000 Experimental evidence of coherence resonance in an optical system *Phys. Rev. Lett.* **84** 3298
[23] Lindner B and Schimansky-Geier L 2000 Coherence and stochastic resonance in a two-state system *Phys. Rev.* E **61** 6103
[24] Dykman M I, Luchinsky D G, McClintock P V E, Stein N D and Stocks N G 1992 Stochastic resonance for periodically modulated noise intensity *Phys. Rev.* A **46** R1713
[25] Qian M, Wang G and Zhang X 2000 Stochastic resonance on a circle without excitation: physical investigation and peak frequency formula *Phys. Rev.* E **62** 6469
[26] Pikovsky A S and Kurths J 1997 Coherence resonance in a noise-driven excitable system *Phys. Rev. Lett.* **78** 775
[27] Liu X, Liu H, Yang J, Litak G, Cheng G and Han S 2017 Improving the bearing fault diagnosis efficiency by the adaptive stochastic resonance in a new nonlinear system *Mech. Syst. Signal Process.* **96** 58–76
[28] Saikia S 2014 The role of damping on stochastic resonance in a periodic potential *Physica* A **416** 411
[29] Huang D, Yang J, Zhang J and Liu H 2018 An improved adaptive stochastic resonance method for improving the efficiency of bearing faults diagnosis *Proc. Inst. Mech. Eng.* C **232** 2352–68
[30] Lu S, He Q and Kong F 2014 Note: on-line weak signal detection via adaptive stochastic resonance *Rev. Sci. Instrum.* **85** 066111
[31] Lu S, He Q, Zhang H and Kong F 2015 Enhanced rotating machine fault diagnosis based on time-delayed feedback stochastic resonance *J. Vib. Acoust.* **137** 051008
[32] Li Y, Zhang B, Liu Z and Zhang Z 2014 Adaptive stochastic resonance method based on quantum particle swarm optimization *Acta Phys. Sin.* **63** 36–43 (in Chinese)
[33] Omkar S N, Khandelwal R, Ananth T V S, Narayana Naik G and Gopalakrishnan S 2009 Quantum behaved particle swarm optimization (QPSO) for multi-objective design optimization of composite structures *Expert Syst. Appl.* **36** 11312–22
[34] Ichiki A and Tadokoro Y 2013 Signal-to-noise ratio improvement by stochastic resonance in moments in non-dynamical systems with multiple states *Phys. Lett.* A **377** 185–8
[35] Ushakov O V, Wünsche H-J, Henneberger F, Khovanov I A, Schimansky-Geier L and Zaks M A 2005 Coherence resonance near a Hopf bifurcation *Phys. Rev. Lett.* **95** 123903
[36] Kiss I Z, Hudson J L, Santos G J E and Parmananda P 2003 Experiments on coherence resonance: noisy precursors to Hopf bifurcations *Phys. Rev.* E **67** 035201
[37] Zhang J, Yang J, Liu H and Zhou D 2018 Improved SNR to detect the unknown characteristic frequency by SR *IET Sci. Meas. Technol.* **12** 795–801
[38] Antoni J and Randall R B 2003 A stochastic model for simulation and diagnostics of rolling element bearings with localized faults *J. Vib. Acoust.* **125** 282–9
[39] Yu D, Cheng J and Yang Y 2005 Application of EMD method and Hilbert spectrum to the fault diagnosis of roller bearings *Mech. Syst. Signal Process.* **19** 259–70
[40] Rai A and Upadhyay S H 2016 A review on signal processing techniques utilized in the fault diagnosis of rolling element bearings *Tribol. Int.* **96** 289–306